FINAL SCIENTFIC AND TECHNICAL REPORT

Project Title: Capillary-Pumped Passive Reactor Concept for Space Nuclear Power

Covering Period: July 7, 2004 through December 31, 2007

Date of Report: May 30, 2008

Recipient:
The Pennsylvania State University
Applied Research Laboratory
North Atherton Street
State College, PA 168084-0030

Award Number: DE-FG07-04ID14590

Subcontractors: N/A

Other Partners: N/A

Contact(s):

Dr. Thomas F. Lin, PI
814-863-4249
ojd@psu.edu

Dr. Thomas G. Hughes, Co-PI
814-865-3418
tgh@psu.edu

Christopher G. Miller, Graduate Assistant
814-777-1805
cgm124@psu.edu

Project Team:
DOE Project Officer: Nancy Elizondo
DOE-HQ contact: Alice Caponiti, Jack Wheeler

Project Objective: To develop the passively-cooled space reactor concept using the capillary-induced lithium flow, since molten lithium possesses a very favorable surface tension characteristic. In space where the gravitational field is minimal, the gravity-assisted natural convection cooling is not effective nor an option for reactor heat removal, the capillary induced cooling becomes an attractive means of providing reactor cooling.

Background: The performing organization of this research program, the Applied Research Laboratory (ARL) of Penn State, has developed a legacy technology to continuously wick molten lithium and achieve sustained liquid metal combustion. The similar capillary wicking phenomenon is applied as the basis of this proposed space reactor concept which has a unique passive safety for cooling. Further important finding of this project is that this reactor concept works very well as a passively safe advanced burner reactor (ABR) for the GNEP endeavor.

Final Status Report:

The final status of this program is reported in the following four areas: (1) A summary of the accomplishment to date, (2) Real-time graphic display data acquisition system for the internally heated and instrumented experiments, (3) Internally heated and instrumented dry-run results with isopropanol, and (4) Conclusion and recommendation for future works, as summarized next. Results of this project to date are promising. While funding were expended before the actual lithium wicking tests could be executed in the most realistic conditions, *i.e.* the internally heated and instrumented heater rods with varying wick structures, all preliminary tests indicated that the lithium tests will be successful as planned. It is believed this technology is profoundly important not only for the passively safe space nuclear power system (as originally proposed), but also for the passively safe advanced burner reactor (ABR) development for the GNEP endeavor. Thus, we intend to carry out such internally heated and instrumented lithium wicking tests with ARL-Penn State's own resources.

1. Summary

Unheated wicking experiments

Unheated wicking experiments were conducted using four different annular wicks of ID 9.525 mm and three different high surface tension liquids, summarized in Table I and Table II, respectively. High surface tension liquids were of interest due to the positive relationship between surface tension and the wicking height of a fluid, generalized by the capillary force balance equation, which is derived from a balance of the pressure difference across the liquid-vapor interface in a wick structure due to surface tension forces with the hydrostatic pressure of the liquid due to gravity. This is expressed in equation form as

$$h = \frac{2\sigma}{\rho g r_e} \quad (1)$$

where h is the wicking height of the fluid, σ is liquid surface tension, ρ is liquid density, g is gravitational acceleration, and r_e is the effective pore radius of the wick structure. In addition to a positive relationship between surface tension and wicking height, Eq. 1 demonstrates an inverse relationship between wicking height and density, gravity, and effective pore radius. Thus, fluids with a high ratio of surface tension to density are expected to wick more vigorously than those with a low ratio of surface tension to density, while wicks with small pores are expected to facilitate wicking better than those with large pores.

The results of the unheated wicking experiments are summarized in Table III, where the predicted wicking heights were calculated using Eq. 1. Though isopropanol had the lowest ratio of surface tension to density of any of the fluids studied, it consistently reached the greatest wicking height. In addition, isopropanol was the only fluid for which wetting was observed on the outer surfaces of the wicks, suggesting that the ability of the fluid to wet the wick structure played a greater role in determining the final wicking height than the surface tension to density ratio. Isopropanol also consistently reached the greatest percentage of its predicted wicking height, though all fluids generally did not approach a large percentage of predicted height, most likely due to the general nature of Eq. 1. However, the trend that was clearly evident for all

fluids was that of decreasing wicking height with increasing pore size, which is consistent with Eq. 1.

TABLE I

Wicks Used in Unheated Wicking Experiments

Wick	Thread Diameter (mm)	Mesh (Threads per Inch)	Pore Diameter (mm)	Material	OD (mm)	Length (m)
A	0.06096	200x600	0.026	SS 304L	14.732	0.3048
B	0.05842	200x200	0.06858	SS 304	14.605	0.5588
C	0.11430	100x100	0.1397	SS 316	14.986	0.5588
D	0.19050	50x50	0.3175	SS 304	14.351	0.5588

TABLE II

Properties of Fluids Used in Unheated Wicking Experiments at 298.15 K

Fluid	Density (kg/m^3)	Surface Tension x 10^3 (N/m)	Viscosity x 10^3 (Pa·s)	σ/ρ x 10^6 ($N \cdot m^2/kg$)
Isopropanol	780	20.93	2.038	26.83
De-Ionized Water	997	71.99	0.89	72.21
Glycerol	1261	62.5	934	49.56
50/50 Glycerol/De-Ionized Water	1129	67.15	Unknown	59.48

Another interesting observation was that, although the wicks with smaller pores tend to wick higher as predicted, they take longer time to reach their final equilibrium heights. This phenomenon could be explained as follows. The wick structure with small pores represents more torturous flow paths for the fluid to reach its final state, thus requires longer time for the equilibrium to be reached. The completion of the unheated wicking experiments serves as the precursor for the externally- and internally-heated lithium wicking experiments.

TABLE III

Comparison of Unheated Wicking Experimental Results with Predicted Results

Fluid	Wick	Predicted Equilibrium Wicking Height (m)	Average Measured Wicking Height (m)	Percent of Predicted Equilibrium Height
Isopropanol	A	0.4211	0.0794	18.86
	B	0.1597	0.0778	48.72
	C	0.0784	0.0572	72.96
	D	0.0345	0.0333	96.52
De-Ionized Water	A	1.1336	0.0699	6.17
	B	0.4298	0.0460	10.70
	C	0.2108	0.0206	9.77
	D	0.0928	0.0048	5.17
50/50 Glycerol/	A	0.7780	0.0508	6.53
De-Ionized Water	B	0.3540	0.0349	9.86
	C	0.1737	0.0159	9.15
	D	0.0765	0.0032	4.18

Externally Heated Lithium Wicking Experiments

Conduction of externally heated lithium wicking experiments required construction of a test apparatus that accommodated temperatures in excess of 1000 K, allowed maintenance of a controlled atmosphere through vacuum sealing, enabled the wick structures to be inserted into and removed from a pool of liquid lithium under such temperature and atmospheric conditions, and allowed observation of the wicking process throughout an experiment. To allow such experiments to be conducted, the test apparatus shown in Figure 1 was constructed.

The test apparatus consists of a quartz cylinder sealed on both ends with aluminum plates and O-Ring seals to serve as a vacuum chamber. The bottom aluminum plate is elevated and includes several sealed fittings to allow electrical connections, instrumentation, and a vacuum line to penetrate the chamber. The top plate includes sealed fittings for an argon line and for a rod which is used to support four wicks inside the chamber, which can be raised and lowered by filling the chamber with argon and loosening the seal to allow movement of the rod. A lithium cup is elevated from the bottom plate inside the chamber to provide room for electrical connections and instrumentation, and is wrapped with a band heater to heat the lithium. Thermocouples allow monitoring of temperature inside of the wick structures and in the lithium pool. Three threaded rods connect the top and bottom plates and are placed in tension to compress the O-Ring seals and seal the chamber. The top plate is well insulated to protect

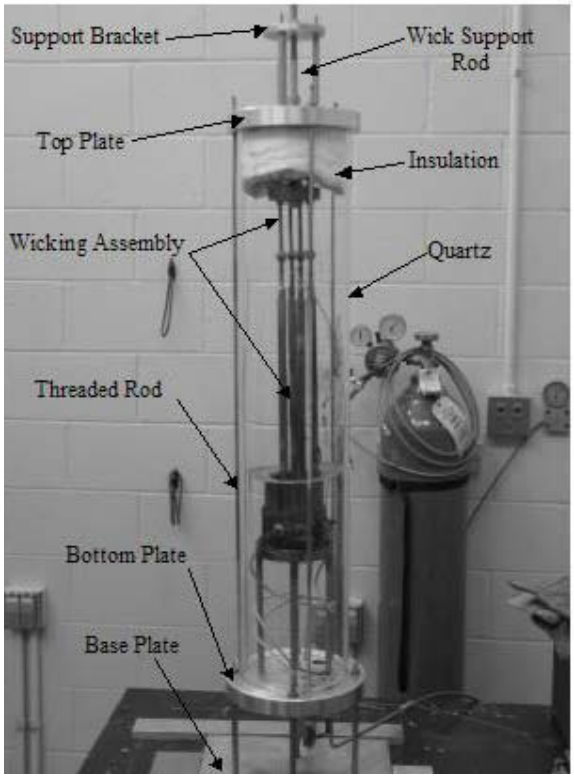

Figure 1: Externally heated lithium test apparatus

against corruption of the O-Ring due to extreme temperatures, and the quartz is surrounded by several 725 W infrared heaters to maintain elevated temperatures inside the chamber and prevent the lithium from returning to its solid state as it wicks away from the hot pool.

Prior to conduction of an externally heated lithium wicking experiment, the lithium was placed in the chamber at room temperature, and the wicks were suspended above the lithium pool. After the chamber was fully assembled, the atmosphere was purged through several iterations of drawing a vacuum followed by back filling the chamber with argon. Prior to testing, the chamber was returned to a vacuum.

Once the final vacuum was drawn, the lithium was melted with the band heater and the entire chamber was heated with the infrared heaters. Once the lithium had reached a liquid state, the chamber was pressurized with argon, and the wick support rod seal was loosened to allow the wicks to be lowered into the lithium, after which the seal was tightened and the chamber atmosphere was purged once again. This was necessary to prevent a reaction between lithium and air, which is particularly volatile when lithium is at an elevated temperature.

Upon completion of an experiment, the wicks were removed from the liquid lithium and the entire test apparatus was allowed to cool to room temperature, at which point it was no longer at risk to expose lithium to the open atmosphere. The wicks were then removed from the chamber and placed in water, which reacts with the lithium to produce hydrogen and lithium

hydroxide. This served the dual purpose of cleaning the wicks and allowing the wicking height of the lithium to be determined by observing hydrogen bubble formation on the wick, as shown in Figure 2.

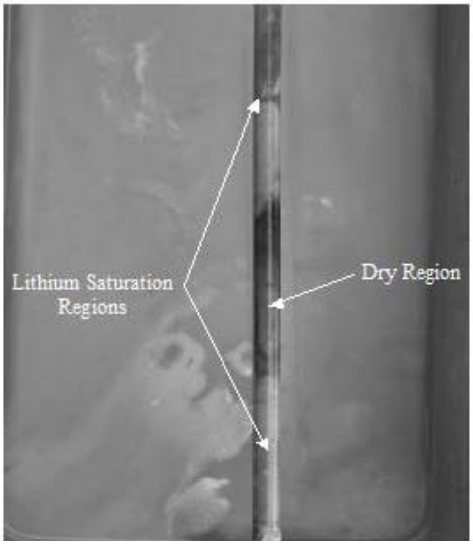

Figure 2: Post-experiment wick cleaning

Four wicks were used in the externally heated experiments, summarized in Table IV. Of particular note is the replacement of two screen mesh wicks with two wicks constructed of sintered metal powder.

It was found from conduction of the externally heated experiments that evaporation of the lithium from the wick structures resulting in complete dry out of the wicks was a major issue in the reduced pressure environment. Thus, it was necessary to conduct the experiments at temperatures substantially below the boiling point of lithium at one atmosphere to prevent the lithium from vaporizing completely as it climbed up the wick. Wick temperatures were thus held to 755.372 K (900 °F) while the lithium was heated to 838.706 K (1050 °F), which successfully prevented the dry out condition and allowed wicking height measurements to be attained.

The results of the externally heated experiment with suppressed wick temperatures are summarized in Figure 3. The greatest wicking height was observed in the 2 micron sintered powder wick, and a trend of decreasing wicking height with increasing pore size was again observed that is consistent with the wicking height equation. Of particular note was the dramatic difference in wicking height between the 20 micron sintered powder wick (F) and the 200x200 screen mesh wick (G). There was a much smaller difference in pore size between Wick F and Wick G than between Wick E and Wick F, but a much larger difference in wicking height. This suggests that the wick structure may play a greater role in wicking height than pore size.

TABLE IV

Wicks Used in Externally Heated Lithium Wicking Experiments

Wick	Structure	Average Pore Diameter (mm)	Material	OD (mm)	Length (m)
E	Sintered Powder	0.002	SS 316	12.7	0.3048
F	Sintered Powder	0.02	SS 316	12.7	0.3048
G	200x200 Mesh	0.0686	SS 304	12.7	0.3048
H	100x100 Mesh	0.1397	SS 316	12.7	0.3048

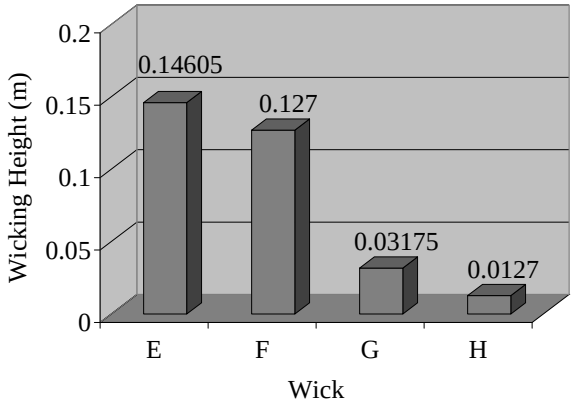

Figure 3: Externally heated experiment results

2. Real-time graphic display data acquisition system

A real-time graphic display of thermocouple data has been integrated with the test apparatus. The display includes a graphic representation of the four wicks, with windows at each of the six thermocouple locations on each wick which display the temperature at each location in real time. One additional window is included in the lithium pool to allow real time display of the lithium pool temperature. Figure 4 shows this display, with room temperature values displayed in the temperature windows. This effort was devoted to facilitate rapid,

computerized, and accurate data acquisition and comprehensive viewing of the test states for the internally heated and instrumented heater rod experiment with lithium wicking.

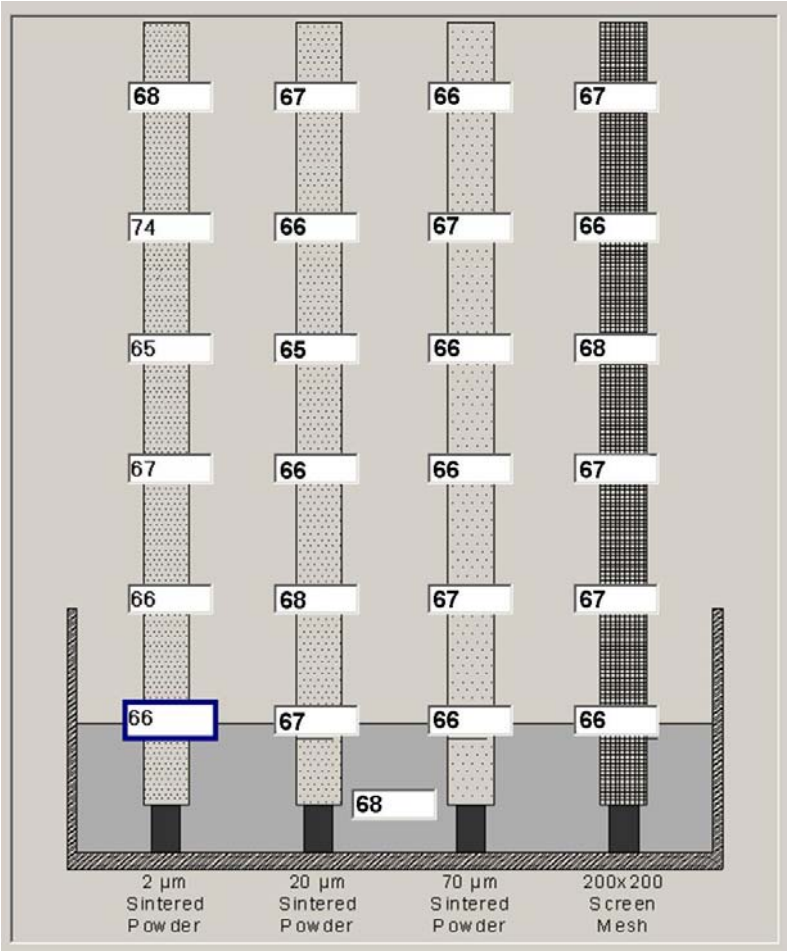

Figure 4: Real time graphic wick temperature display

In addition to the real time display the system allows for recording of the data from each thermocouple for detailed data analysis following testing. Figure 5 shows this recording interface, which also displays all thermocouple temperatures in real time and plots up to 6 real time temperatures for a real time temperature history. However, before we actually conduct the internally heated and instrumented heater rod experiment with lithium wicking, we felt it is necessary to conduct a dry run with a fully instrumented heater rod that heats a pool of isopropanol, along with the other three unheated rods but with their perspective wick structures. This allows us to check the overall system functionality and safety issues before the fully-pledged 4-rod internally heated and instrumented heater rod experiment with lithium. This task has indeed been successfully accomplished, and is discussed next. High degree of confidence for the lithium tests is attained from this dry-run.

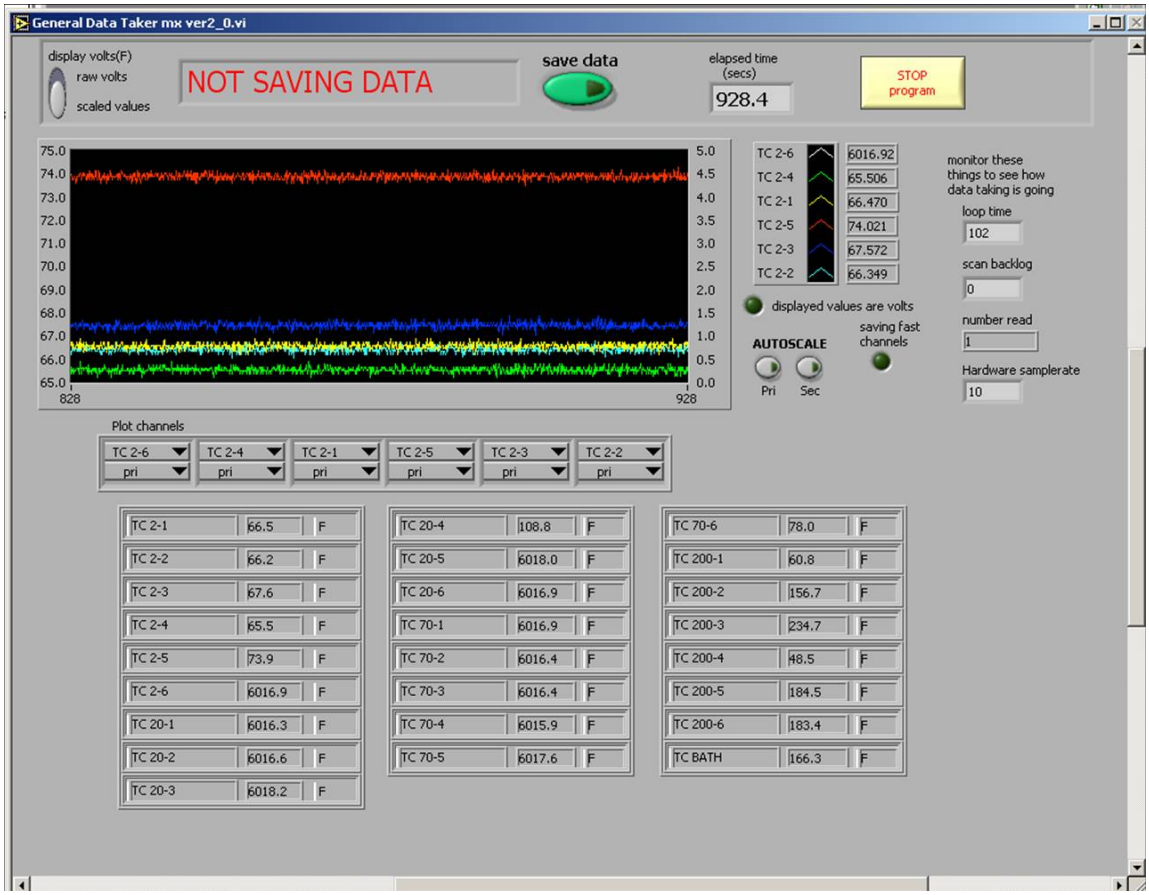

Figure 5: Data recording interface

3. *Internally heated and instrumented dry-run results*

A test of the internally heated configuration was performed using a single fully instrumented heater rod and isopropanol as a wicking fluid. The heater rod was constructed using a molybdenum disilicide ($MoSi_2$) resistance heating element surrounded by high thermal conductivity boron nitride insulation with an outer SS 316 cladding, as shown in Figure 6. The overall length of the heating element was 24 inches, with the heated portion occupying the middle 12 inches. Six grooves in the BN insulation allowed for the internal placement of six thermocouples, detailed in Figure 7, which were evenly spaced along the length of the heated portion of the heating element. The two larger ends of the heating element were covered with high temperature fiberglass sleeving to provide electrical insulation between the heating element and the cladding, as shown in Figure 8.

The heater rod was integrated with the empty cup that is intended for molten lithium by allowing the cladding to penetrate the bottom of the cup, where it was welded in place. Thus, the cup was placed at the beginning of the heated portion of the rod, allowing for future lithium testing along the heated section. Three other stainless steel tubes were also welded through

the cup to allow for future integration of three additional heater rods. Four wick structures were then placed around the tubes, with the fully instrumented heater rod located at the center of a 70 micron sintered powder wick, as shown in Figure 9.

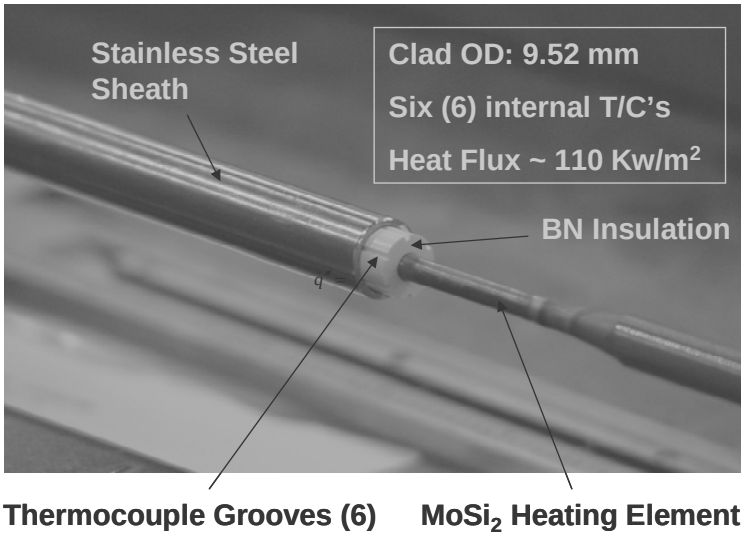

Figure 6: Heater rod assembly detail

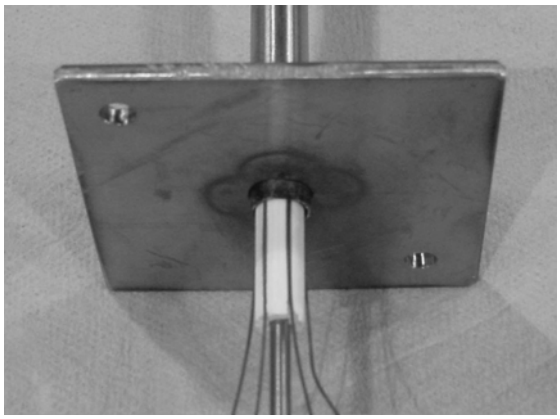

Figure 7: Heater rod thermocouple instrumentation

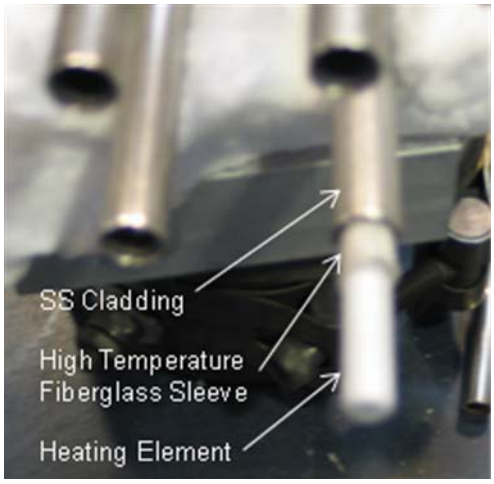

Figure 8: Heater rod end detail

Figure 9: Internally heated test configuration

With the heater rod and wicks in place a test was conducted using isopropanol as the wicking fluid. A steady current of 25 A was supplied to the heater rod, and the temperatures and power were recorded at a sampling rate of 1 Hz. Wicking was observed in each of the

unheated wicks but not in the heated wick, which is likely due to the facilitation of evaporation by providing heat to the wick structure. The results of the test are shown in Figure 10, where TC 70-1 is the thermocouple that was placed 1 in. above the lower end of the heated portion of the heater rod, with TC 70-2 through TC 70-6 successively placed at 2 in. intervals above TC 70-1.

The test verified the successful operation of the heater rod in an internally instrumented experimental configuration. Also apparent from the data was a parabolic or cosine-shape temperature profile in the heater rod, as shown by the peak temperature readings from the thermocouples closest to the center of the rod and the lowest temperature readings at the ends of the rod. Though the run time was not sufficient to reach steady state, the shape of the temperature vs. time plot suggests that the rod may have been approaching a steady state condition. Also of note is the increase in power that can be seen with increasing temperature. This is consistent with prior heater rod testing during which the resistance of the heating element was observed to increase with temperature. Since the current was held constant, the voltage across the heater rod was allowed to vary and thus increased as the resistance of the heating element increased with temperature, resulting in increased power through the heater rod.

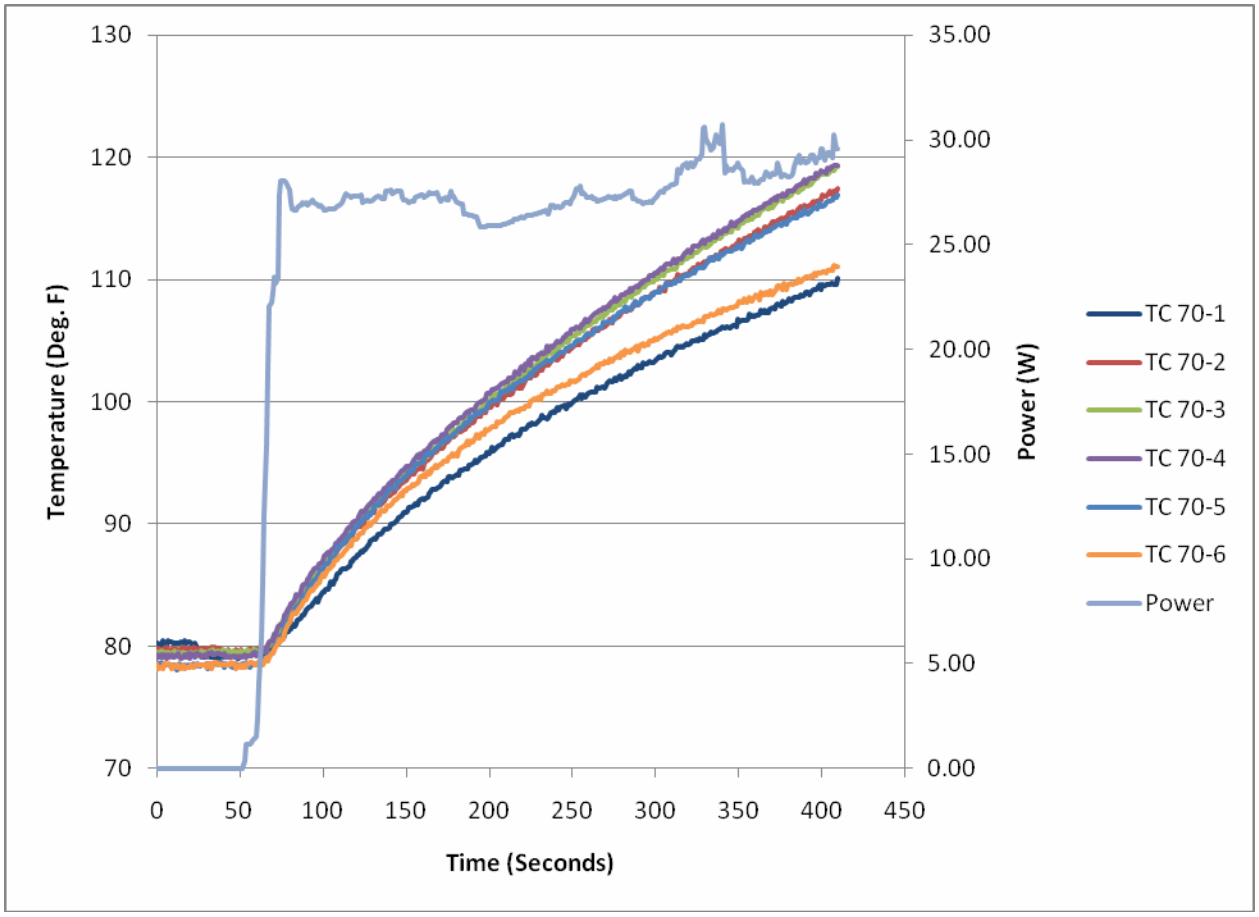

Figure 10: Initial internally heated test results from 70 micron sintered powder wick

4. Conclusion and recommendation for future works

Two major tasks remain to be completed. The first is the conduction of internally heated lithium wicking experiments using the test apparatus with fully integrated heater rods, as illustrated in the configuration of Figure 11 with the automatic motor-driven wick assembly, and the second is the supporting numerical modeling of the wick structure using temperature data obtained from the conduction of the internally heated experiments. Expected completion date for the remaining work, to be supported by ARL-Penn State internal resources, is about the end of summer 2008. One unique advantage of using the $MoSi_2$-based heater rod is the very fact that the heating element's resistivity increases with the temperature. As a constant current is applied through the heater rod, it causes the middle portion of the rod hotter than the edge portion as observed from the dry run. Thus the heater rod exhibits a natural parabolic or cosine-shape axial power profile, peaking at the center. This is ideally suited to simulate the realistic fission power profile of most nuclear fuel rods due the neutron flux distribution.

In conclusion, the concept of a passively-safe, capillary-pumped and cooled reactor system is fundamentally sound, and has been experimentally demonstrated in the externally heated environment, and will be more closely demonstrated in an internally heated and instrumented lithium environment. This concept actually goes far beyond space nuclear power applications. We are currently exploring its application as a passively-safe, capillary-pumped and cooled Advanced Burner Reactor (ABR) system that is critically important for the Global Nuclear Energy Partnership (GNEP) initiative. We named it the Capillary Pumped Advanced Burner Reactor (CPABR).

Figure 11: The motor-driven mechanism to position the wick assembly

Patents: N/A.

Milestone Status Table: The milestone chart below reflects the status of the accomplishment compared against the proposed. Some specific tasks, although not explicitly stated in the original proposal, are also highlighted since they are in the critical path for the completion of the project as planned.

ID Number	Task / Milestone Description	Planned Completion	Actual Completion	Comments
1	Model development	6/30/05	6/30/05	
2	Lithium wicking experiment with quartz tubes (not in the project critical path)	6/30/05		New date 3/15/2007, will be piggy-backed to the planned experiments
3	Assessment of micro-gravity experiments	6/30/05	6/30/05	
4	Year-1 report	6/30/05	10/5/05	**Submitted 10/5/05**
5	Develop computational tools	6/30/06		In progress
6	Evaluate and test different wicks	6/30/06	11/30/05	
7	Design the capillary test rig	6/30/06	12/31/05	
7.1	Thermal simulator (heater rod) design completed		6/30/05	Included in Yr-1 report
8	Year-2 report	6/30/06	11/3/06	**Submitted 11/3/06**
9	Construct and shake down the capillary test rig	9/30/06	6/30/06	Included in Yr-2 report
9.1	Successfully tested the thermal fuel simulator		8/31/05	Included in Yr-1 report
9.2	Test rig build-up - including the completion of unheated and externally heated lithium tests		8/31/06	Included in Yr-2 report
10	Scaling of the passive CPR	12/31/07		In progress
11	Experiment with the capillary test facility (internally heated)	12/31/07		In progress, completed internally heated dry run
12	Year-3 report	7/06/07		**Submitted 10/24/07**
13	Final Scientific and Technical Report	12/31/2007		**Submitted 5/30/2008**

Budget Data (as of date):

			Approved Spending Plan			Actual Spent to Date		
Phase / Budget Period			DOE Amount	Cost Share	Total	DOE Amount	Cost Share	Total
	From	To						
Year 1	7/7/04	7/6/05	$97,038	0	$97,038	$83,400	0	$83,400
Year 2	7/7/05	7/6/06	$96,425	0	$96,425	$90,790	0	$90,790
Year 3	7/7/06	7/6/07	$99,265	0	$99,265	$84,968	0	$84,968
Year 4	7/7/07	9/30/07	0			$20,438	0	$20,438
Year 4	10/1/07	12/31/07	0			$13,132	0	$13,132
		Totals	$292,728		$292,728	$292,728		$292,728

Spending Plan for the Next Year:

None.